Chapter 5

The Sonochemical Functionalization of MoS_2 by Zinc Phthalocyanine and its Visible Light Induced Photocatalytic Activity.

5.1 Introduction

Two-dimensional ($2D$) nanomaterials, such as graphene based materials and transition metal dichalcogenide ($TMDCs$), have been shown to hold great promise in next-generation electronic and optoelectronics applications over the last few years [100, 252-254]. Their exceptional properties such as strong electron-hole confinement, thickness-dependent electronic band structure and high transparency, which are inherited from the ultrathin planar structures allows for the fabrication of thinner, flexible and efficient devices. The large surface area of these $2D$ materials creates an ability to form unique hybrid composites with other optical inorganic or organic nano materials, polymers, metals, organic small molecules etc [255, 256]. Recently few-atom layers of $TMDCs$ like MoS_2, WS_2 etc. have been synthesised and studied a lot for their potential use in electronics [257-259]. Among the mostly explored $TMDCs$ layered materials, single and few layer molybdenum disulphide (MoS_2) materials have drawn immense attention because of their having a direct band-gap [115, 260]. This leads MoS_2 nanosheet as a potential electronic and optoelectronic devices [100, 259]. The Presence of a direct bandgap feature in MoS_2 makes it an outstanding candidate especially for optoelectronic applications, such as photodetector [261, 262], photovoltaics [263, 264] and light emitters [265]. At the same time, the switching ability from the indirect to a direct bandgap leads to the emergence of photoluminescence (PL) which is not seen in the bulk form [266]. In particular, mono or few layers MoS_2 nanosheets has shown great potentiality in optoelectronic and photocatalytic applications by means of its unique structural, electrical

and optical features. The main advantage of MoS_2 is the high melting point, chemical inertness and surface stability at room temperature [267]. It is expected that like graphene, it could be an excellent template for attaching several optical materials towards achieving new hybrid functional materials for efficient photo induced charge generation.

The photocatalytic degradation of hazardous organic pollutants using different nano structured materials including semiconductor, polymer or organic small molecules has attracted extensive attention due to their high photocatalytic efficiency [268-270]. The performance of these optical materials depends on: efficient formation of exciton through light absorption, dissociation of excition to the free charge carriers, transfer of charges from the optical material to the organic pollutant and large exciton diffusion length. But the fast recombination probability of the photogenerated electron-hole is the main drawback of these materials. It is well established that formation of hybrid materials by anchoring optical materials on the surface of carbon-based nano materials like graphene, reduced graphene oxide (RGO), carbon nanotube (CNT), and activated carbon reduces the recombination probability of the charge carriers and that is greatly advantageous in the field of optoelectronic applications [81, 206, 271, 272]. Because of large $2D$ surface area with direct band gap property, mono-layer MoS_2 could be a better matrix element towards forming efficient hybrid optical materials. To this end, metal pthalocyanine (MPc) has enjoyed the driving position owing to its synthetic modification, ultra high electronic delocalization, great photochemical properties and thermal stability [273, 274] . They have shown the ability to make well-ordered thin film and wide absorption range from ul-

tra violet (UV) to visible (vis) region. These properties make MPc's very good candidate in the field of optoelectronic devices like thin film transistors, photo $FETs$, light emitting diodes, solar cells and many other application [273, 274]. Among them, zinc phthalocyanine is considered as a superior candidate in the field of optoelectronics due to its high photo sensitivity, reproducibility, large cross-sectional absorbance in UV-vis region etc.[274]. We have specially chosen tetra-tert-butyl zinc(II) phthalocyanine ($ZnTTBPc$), a solution processable widely used optoelectronic materials which offers ease of material processing with substance suitability, chemical durability with high yield quantum efficiency [275, 276].

Figure 5.1.1: Photo Catalytic degradation mechanism of PNP by $MoS_2 - ZnTTBPc$

In the study presented here, we have successfully synthesized layer structured MoS_2 by simple solvothermal route and funtionalization it by the sonochemical technique with $ZnTTBPc$. As-synthesized $MoS_2 - ZnTTBPc$

hybrid nanocomposite material has been characterized by means of different techniques such as XRD, TEM, AFM, $UV-Vis$, Raman and $FTIR$. To give significant insight into interfacial energy transfer among $MoS_2-ZnTTBPc$ components of the composite, steady state PL and $TCSPC$ study have been employed. Raman study gives sufficient evidence towards the existence of mono-layer MoS_2 in the composite. The photocatalytic activity of the $MoS_2-ZnTTBPc$ composites was investigated under simulated solar light irradiation for the degradation of 4−nitrophenol. It has been found that the photocatalytic efficiency of the composite is enhanced in compared to the controlled counterparts. Furthermore, the possible mechanism involved in the photacatalytic process has also been proposed. The present study opens new possibilities to functionalize MoS_2 by different organic and inorganic optical donor materials, where single layer MoS_2 acts as an acceptor.

5.2 Experimental Section

5.2.1 Materials Used

Sodium molibdate dihydrate $[Na_2MoO_4, 2H_2O]$, thiourea $[SC(NH_2)_2]$, N, N-dimethylmethanamide $[DMF]$, potassium bromide $[KBr]$, 4-nitrophenol $[4-NP]$, sodium borohydride $[NaBH_4]$ were purchased from Sigma-Aldrich. Methanol and ethanol were purchased from Merck. All the chemicals and reagents were of analytical grade and used without further purification.

5.2.2 Material Preparation

5.2.2.1 MoS_2 Synthesis

MoS_2 was synthesized according to the method reported by Lu and other scientists with some modification [277-279]. In a typical method,725 mg (3 $mmol$) of $Na_2MoO_4, 2H_2O$ and 1140 mg (15 $mmol$) thiourea was kept in a conical flux. 30 mL of double distilled (DD) water was added into the flux. Then the solution was stirred for 30 $minutes$ to form a homogeneous solution. The resultant solution was transferred to a Teflon coated autoclave and kept in a preheated furnace ($210°C$) for 24 hours. Then it was cooled to the room temperature normally. A black precipitate of MoS_2 was formed.

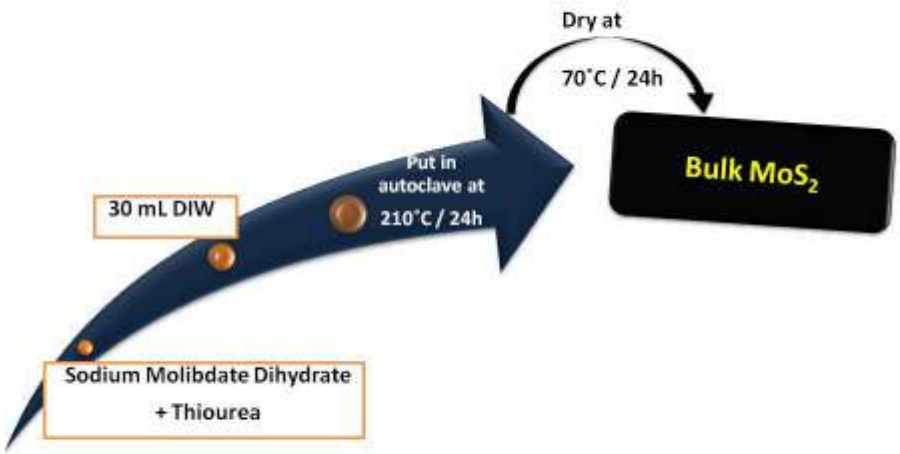

Figure 5.2.1: Synthesis of Bulk MoS_2

It was separated from the solution by centrifugation followed by washing

with DD water and ethanol repeatedly. The black MoS_2 sample was kept in a furnace at $70°C$ for over-night. Single or few-layer MoS_2 was prepared by the exfoliation of MoS_2 by simple ultrasonication in methanol. In a typical process, $750\,mg$ of the as-synthesized MoS_2 particle was taken in a conical flux and dispersed in $15\,ml$ of methanol. The dispersed solution was then ultrasonicated for $2\,hours$ at room temperature in a probe sonicator. Finally, a dark brown suspension was formed and which was subjected to centrifugation (speed $4000\,rpm$) for $10\,min$. The residue was dried at $70°C$ in a furnace for $10\,hrs$. Ultimately, layered-MoS_2 sample was formed and collected for further study.

Figure 5.2.2: Synyhesis of mono or few layer MoS_2

5.2.2.2 Synthesis of $MoS_2 - ZnTTBPc$ nano composite

Sonochemistry technique has been adopted for the attachment of small $ZnTTBPc$ molecule on the surface of MoS_2 and formation of $MoS_2 - ZnTTBPc$ hybrid material. In a beaker, $10\,mg$ of MoS_2 powder was dissolved in $10ml$ DMF solvent by $30\,min$ ultrasonication. In another beaker $ZnTTBPc$ ($10\,mg$) was dissolved in $10\,ml$ of DMF solvent. A homogenous dark blue $ZnTTBPc$ solution was prepared by $30\,min$ stirring. The solution of MoS_2 and $ZnTTBPc$

were mixed in the weight ratio of 1 : 1 and the resultant mixture was ultrasonicated in a probe sonicator for 300 *minutes*. The color of the solution changed from dark blue to blackish blue. Then it was centrifuged several times and then dried in a vacuum chamber for overnight. Thus synthesized $MoS_2 - ZnTTBPc$ composite is designated here as $MoS_2 - ZnTTBPc$ $(1:1)$. A set of $MoS_2 - ZnTTBPc$ nanocomposites with different weight ratio of MoS_2, keeping $ZnTTBPc$ as constant $(1:1,\ 2:1,\ 3:1, 4:1\ and\ 5:1)$ were synthesized.

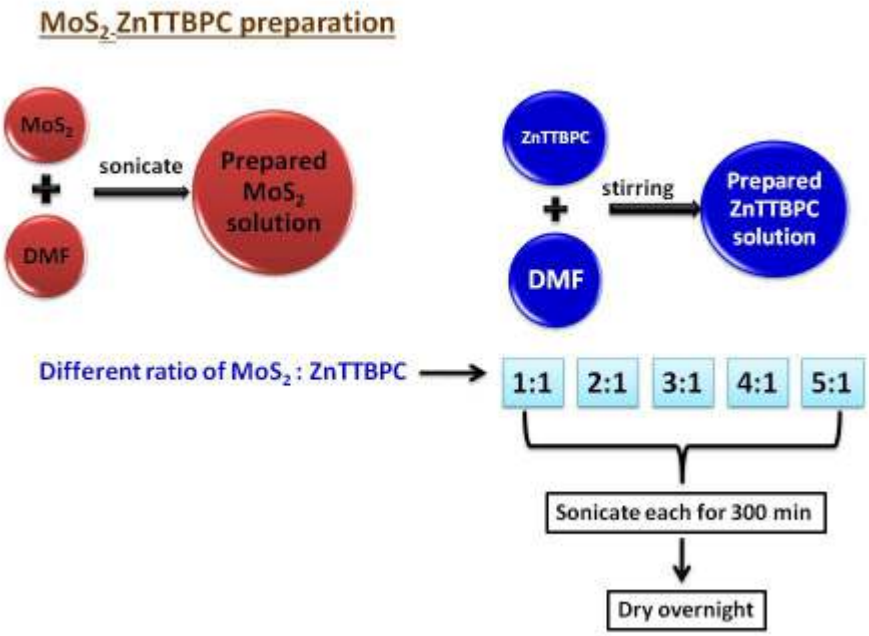

Figure 5.2.3: Synthesis of $MoS_2 - ZnTTBPc$ nano composite (Different weight ratio)

5.3 Material Characterisation

In order to characterize the crystalline structure of the as-synthesized materials, X-ray diffraction (XRD) study was performed. The diffraction patterns were recorded using an X-ray diffractometer (Rigaku Miniflex 600) with Cu K_α radiation($= 1.5406\mathring{A}$) at a scan rate $10^\circ/min$, operating voltage $40\,kV$. Transmission electron microscope (TEM) and high resolution TEM ($HRTEM$) images were obtained with a JEOL – JEM 2100 F electron microscope operated at $200\,kV$. $UV-vis$ absorption spectra of controlled-MoS_2, controlled-$ZnTTBPc$ and $MoS_2-ZnTTBPc$ composite (in DMF solvent) were recorded with a spectrometer (Shimadzu $UV-1700$). Room temperature steady-state photoluminescence (PL) measurements were carried out with the help of a spectrofluoro photometer (Perkin Elmer LS 55) with excitation wavelength of $540\,nm$. The time-resolved fluorescence experiment in nanosecond range were carried out using time-correlated single photon counting ($TCSPC$) setup (Delta Flex Modular Fluorescence Lifetime System, Delta diode HORIBA Scientific (model no $DD-415L$); and a Laser diode radiation of Excitation wavelength $540\,nm$ was used for excitation. A Fourier transform infrared ($FTIR$) spectrometer (Perkin Elmer - Spectrum 100) was used for recording of transmittance spectrum of our sample in the range of $400\,to\,4000\,cm^{-1}$. Raman scattering measurement was carried out at room temperature on a confocal lens triple micro Raman spectroscopy (Jobin-Yvon Horiba model: $T64000$) equipped with an Argon diode laser source of excitation wavelength $514\,nm$

5.4 Evaluation of Photo Catalytic Reduction of $4-NP$

To investigate the photocatalytic performance, degradation of $4-NP$ in presence of excess amount of $NaBH_4$ under the simulated solar light irradiation was considered as a model reaction. The concentration of $4-NP$ was computed by recording the absorption peak intensity at $422\,nm$. Usually, $5\,ml$ of $4-NP$ ($0.03\,mM$) was added with the excess amount of $NaBH_4$ ($6\,ml$ of $0.1\,M$ concentration). In room temperature, $200\,\mu L$ of photocatalyst solution ($1\,mg/1\,ml$) was added under the stirring condition and continued for another $12\,minutes$ to reach the adsorption-desorption equilibrium state. Then the solution was exposed under a solar light simulator (Oriel 67005, Newport, $AM\,1.5$) with an intensity of $100\,mW/cm^2$. The photocatalytic reaction starts immediately after the shining of light. The photocatalytic activity was evaluated from the decrement of the intensity of the phenolate ion at $422\,nm$ with a constant time interval of solar light irradiation.

5.5 Result and Discussion

5.5.1 Structure and Morphology Study

XRD patterns of the controlled-MoS_2, controlled-$ZnTTBPc$ and $MoS_2-ZnTTBPc\,(3:1)$ nanocomposites are compared in Figure 5.5.1A. For the controlled-MoS_2 all the peaks observed at 14.2, 33.5, 39.8, 43.1, 49.1 and 59.3° are corresponding to (002), (100), (103), (006), (105) and (110) planes

respectively and indexed as hexagonal phase of MoS_2 (JCPDS Card No. $b37 - 1492$). The most significant and strong peak, appeared at $14.42°$ confirms the layered structure of MoS_2 [280, 281]. In the XRD pattern of $MoS_2 - ZnTTBPc$ all the peaks related to layered-structure MoS_2 are present. Apart from these, two new peaks appeared at $5.04°$.and $6.72°$. These two most pronounced peaks of $ZnTTBPc$ arise mainly because of β-polymorph of $ZnTTBPc$ and signify (100) and (110) plane [81, 275]. The absence of additional peaks confirms the crystalline alignment of MoS_2 layered structure is not modified by the attachment of $ZnTTBPc$ and vice-versa.

For better understanding the microscopic properties, $HRTEM$ imaging of the sonochemically (sonication time $300\,min$) synthesized $MoS_2 - ZnTTBPc$ $(3:1)$ composite was carried out and an image is presented in Figure 5.5.1B. The $HRTEM$ image clearly shows the periodic arrangement of atoms and the interplanar spacing is $0.27\,nm$ which perfectly matches with the (100) plane of MoS_2.

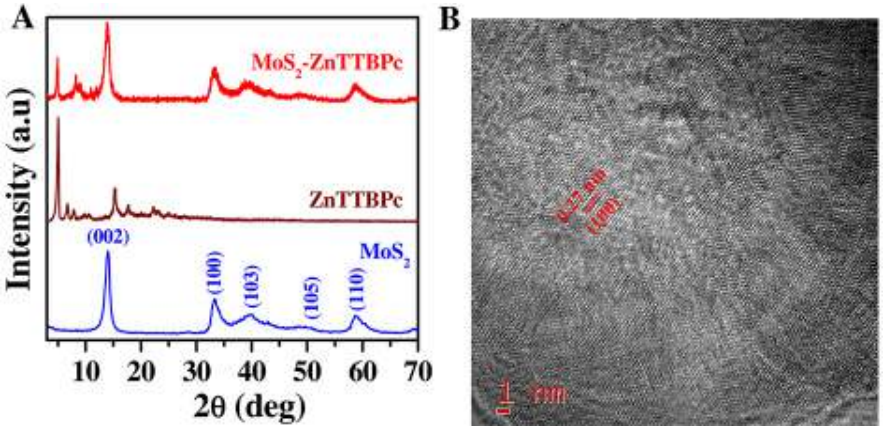

Figure 5.5.1: (A) XRD patterns of MoS_2, $ZnTTBPc$, and $MoS_2 - ZnTTBPc$ $(3:1)$ composite. (B) $HRTEM$ image of $MoS_2 - ZnTTBPc$ $(3:1)$ composite.

5.5.2 Optical Absorption Study

The steady-state $UV - vis$ absorption spectroscopy was used towards a better understanding of the electronic interaction among $ZnTTBPc$ small molecules and MoS_2 layers. Figure 5.5.2A compares the optical absorption spectra of controlled-$ZnTTBPc$, controlled-MoS_2 and $MoS_2 - ZnTTBPc$ $(3:1)$ composite. In the absorption spectra of controlled-$ZnTTBPc$, two groups of intense absorption peaks are observed. One is at $676\,nm$, Q band due to HOMO-LUMO ($\pi \rightarrow \pi^*$) transition and another is at $348\,nm$ (Soret band or B band) [272]. In the absorption spectrum of MoS_2 (inset of Figure 5.5.2A), two humps at $620\,nm$ and $670\,nm$ are observed. These are the consequent of transition among valence band (VB) and conduction band(CB) of MoS_2.

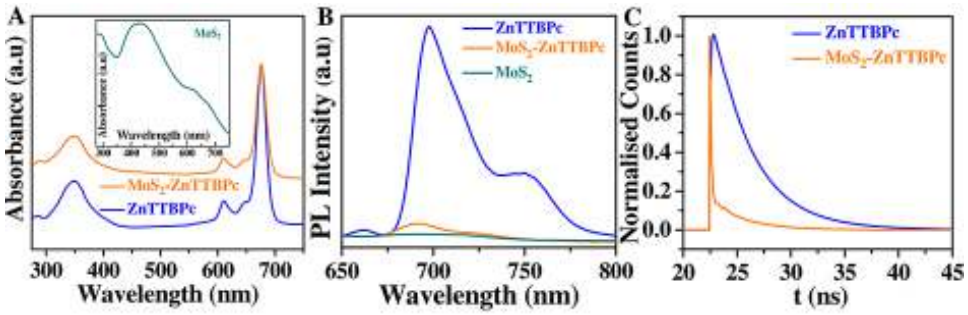

Figure 5.5.2: (A) Optical absorption spectra of controlled-$ZnTTBPc$ and $MoS_2 - ZnTTBPc$ $(3:1)$ composite. The optical absorption of controlled-MoS_2 is shown in the inset of (A). (B) Photoluminescence spectra of controlled-$ZnTTBPc$, controlled-MoS_2, and $MoS_2 - ZnTTBPc$ $(3:1)$ composite. (C) Lifetime transients of controlled-$ZnTTBPc$, and $MoS_2 - ZnTTBPc$ $(3:1)$ composite.

We have also studied $UV-vis$ absorption spectra of $MoS_2-ZnTTBPc$ composites such as $MoS_2 - ZnTTBPc\,(1:1)$, $MoS_2 - ZnTTBPc\,(2:1)$, $MoS_2 - ZnTTBPc\,(3:1)$, $MoS_2 - ZnTTBPc\,(4:1)$ and $MoS_2 - ZnTTBPc\,(5:1)$ and compared with that of controlled-$ZnTTBPc$ in Figure 5.5.3. We have studied the $UV-Vis$ absorption spectra with the variation of sonication time for all the composites to give significant insight into the effect of sonication time on the degree of interaction among $ZnTTBPc$ and MoS_2 layers. It is noticed that for all the cases the peak of the B-band of $ZnTTBPc$ at $348\,nm$ is blue shifted and appears broadened gradually with the sonication time and ultimately fixed at $340\,nm$ after $300\,min$ of ultrasonication. Blueshift of the peak confirms the π-electronic interaction between the acceptor MoS_2 nanosheets and the donor $ZnTTBPc$ molecules [81]. It is also observed that for the $MoS_2 - ZnTTBPc$ family members, the absorption in the region of $300-800\,nm$ has increased compared to controlled-$ZnTTBPc$ that may facilitate the enhancement of photo-induced

charge generation in the composite.

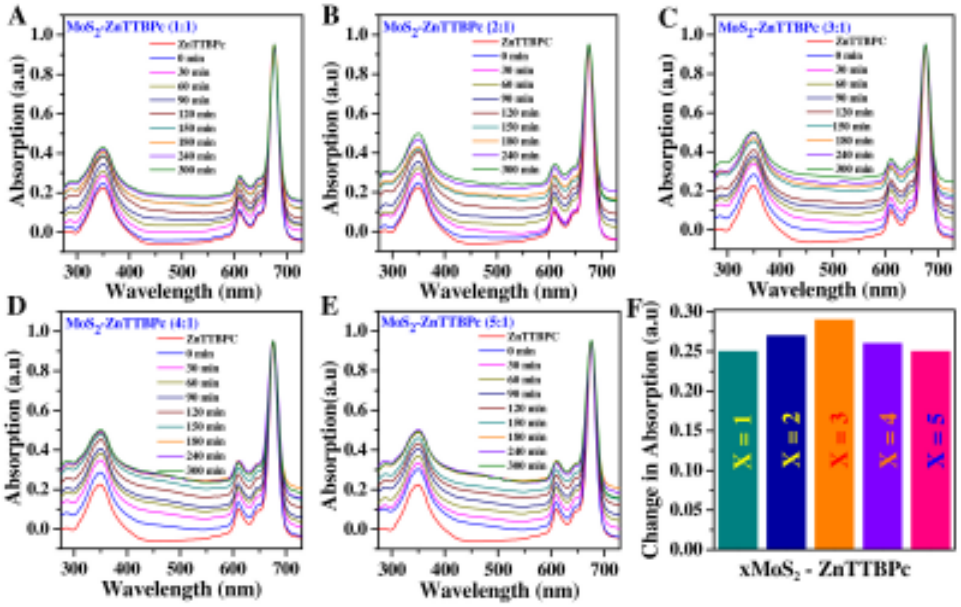

Figure 5.5.3: Optical absorption spectra of $MoS_2 - ZnTTBPc$ composite with varying ratio of MoS_2 *and* $ZnTTBPc$ (A) 1 : 1, (B) 2 : 1, (C) 3 : 1, (D) 4 : 1, (E) 5 : 1. (F) A comparison of change in absorption after300 min of sonication for the varying ratio of MoS_2 in the $MoS_2 - ZnTTBPc$ composite.

5.5.3 Steady State Photoluminescence and Lifetime Study

The significant electronic interaction between the MoS_2 and $ZnTTBPc$ in the $MoS_2 - ZnTTBPc$ hybrid material was further established by a photoluminescence (PL) study. The steady-state room temperature PL spectra of $ZnTTBPc$ small molecules after successive attachment of MoS_2 with different ratios are shown in Figure5.5.4.The PL emission spectra of controlled-$ZnTTBPc$, controlled MoS_2 and $MoS_2 - ZnTTBPc\,(3:1)$ are compared in Figure 5.5.2B. As shown in the figure, $ZnTTBPc$ has a strong emission with maximum intensity at 697.5 nm. A significant quenching of PL

intensity is observed for all the $MoS_2 - ZnTTBPc$ composites. It is also observed that the intensity of PL of $ZnTTBPc$ decreases with an increase in the concentration of MoS_2, which confirms that the quenching is only due to the presence of MoS_2 nanosheets. A remarkable quenching of emission of $ZnTTBPc$ signifies the occurrence of photo-induced efficient charge or energy transfer through the interface of $ZnTTBPc$ and MoS_2. The energy transfer efficiency (E) can be approximated from the equation given below [282]:

$$E = 1 - \frac{F_{DA}}{F_D} \tag{5.5.1}$$

where F_D is the PL intensity of $ZnTTBPc$ in absence of MoS_2 (acceptor), and F_{DA} is the PL intensity of $ZnTTBPc$ in presence of MoS_2 (acceptor). The value of E were found to be 61, 73, 91, 90 and 89% for $MoS_2 - ZnTTBPc$ hybrid material of different ratios (1 : 1), (2 : 1), (3 : 1), (4 : 1) and (5 : 1) respectively. Thus the quenching efficiency reaches a maximum value($\sim$ 91%) for the $MoS2 - ZnTTBPc(3 : 1)$ composite; beyond it, quenching efficiency decreases with the further increase of MoS_2 contain in the composite. Furthermore, A clear blue shift of the emission peak of $ZnTTBPc$ at $697.5\,nm$ is observed after successive attachment of MoS_2 due to the strong electronic interaction of $ZnTTBPc\ and\ MoS_2$ [283]. The singlet extited state photo-illuminated $ZnTTBPc$ donor molecules can transfer photo-induced electrons to the acceptor MoS_2 sheets in the $MoS_2 - ZnTTBPc$ composite. Similar charge transfer interaction is observed in different phthalocyanine- based composite systems. To investigate the quenching nature of the $MoS_2 - ZnTTBPc$ composite time-correlated single pho-

ton counting technique ($TCSPC$) at room temperature was employed and LED source having a wavelength of $540\,nm$ was used as an excitation source. It was observed that the fluorescence (FL) lifetime of $ZnTTBPc$ small molecule decays in presence of MoS_2 nanosheets. The distinctive time-resolved PL ($TCSPC$) lifetime decay spectra of $ZnTTBPc$ molecules and $MoS_2 - ZnTTBPc\,(3:1)$ nanocomposite is shown in Figure 5.5.2C. Here it is observed that the $MoS_2 - ZnTTBPc\,(3:1)$ decay curve is steeper than that of control $ZnTTBPc$. The average lifetime of $ZnTTBPc$ in the absence and in presence of MoS_2 layered sheet was estimated analytically by the empirical expression given below [282] :

$$\tau(ave) \quad = \quad \frac{\sum_{i=1}^{n} A_i \tau_i}{\sum_{i=1}^{n} A_i} \tag{5.5.2}$$

where, n is the number of discrete decay components, τ_i decay times, and A_i gives the weighing parameter associated with the i^{th} decay. It was found that the average FL decay lifetime of pure $ZnTTBPc$ is $13.72\,ns$ and that of the $MoS_2 - ZnTTBPc\,(3:1)$ nanocomposite is $1.45\,ns$. So with the anchoring of $ZnTTBPc$ molecules on $2D{-}MoS_2$ nanosheet the FL intensity as well as decay lifetime decreases. The shorter lifetime leads towards the energy transformation from $ZnTTBPc$ to MoS_2. The quenching of peak intensity in PL as well as decreasing FL life time in $TCSPC$ study jointly validates the electronic energy transfer at the interface of MoS_2 layer and $ZnTTBPc$.

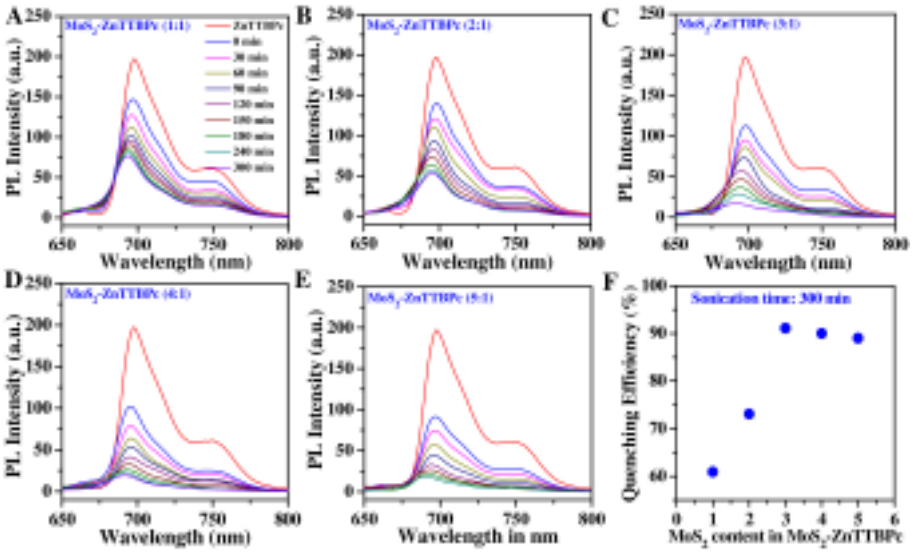

Figure 5.5.4: Photoluminescence spectra of controlled-$ZnTTBPc$, and $MoS_2 - ZnTTBPc$ composite with varying ratio of MoS_2 and $ZnTTBPc$ (A) $1:1$, (B) $2:1$, (C) $3:1$, (D) $4:1$, (E) $5:1$. (F) Variation of quenching efficiency of the $MoS_2 - ZnTTBPc$ composite for different MoS_2 content in the composite after $300\,min$of sonication.

The optoelectronic energy transfer efficiency through the interface between MoS_2 and $ZnTTBPc$ for the composite can be estimated from the expression given below [282]:

$$E = 1 - \frac{\tau_{DA}}{\tau_D} \tag{5.5.3}$$

where, τ_{DA} and τ_D denotes the FL decay lifetime concerned with $MoS_2 - ZnTTBPc\,(3:1)$ nanosheet and $ZnTTBPc$ respectively. The calculated energy transfer efficiency of $MoS_2 - ZnTTBPc\,(3:1)$ nano composite is 90% which is almost equal to the value calculated from the steady-state PL Study.

5.5.4 FTIR and Raman Study

Figure 5.5.5A compares the $FTIR$ spectra of controlled-$ZnTTBPc$, controlled-MoS_2 and $MoS_2-ZnTTBPc\,(3:1)$ composite. $FTIR$ spectra of controlled-$ZnTTBPc$ display the characteristic fingerprint of $ZnTTBPc$ at 1045–1612 cm^{-1}. The significant peak at 747 cm^{-1} is attributed to $C-H$ out of plane deformation [284]. The peaks at 902 cm^{-1} and 1259 cm^{-1} are mainly due to bending and stretching modes of $C-N$ bond. The peak at 1092 cm^{-1} is attributed to the PC skeletal vibration. A set of peaks at 1394 cm^{-1}, 1495 cm^{-1} and 1612 cm^{-1} ascribed as stretching of phenol ring, stretching pyrol ring and stretching benzene ring, respectively. The peaks for $C-H$ stretching of $ZnTTBPc$ molecules are located in the range of 2856 cm^{-1} to 2956 cm^{-1} [275]. A weak peak at 467 cm^{-1} is observed due to the $Mo-S$ stretching vibration mode of MoS_2 [285]. All the significant range of peaks of $ZnTTBPc$ and the peak for $Mo-S$ stretching clearly co-existed in the $FTIR$ spectra of $MoS_2-ZnTTBPc$ (in all ratios) nanocomposite which firmly confirms the formation of $MoS_2-ZnTTBPc$ hybrid composites.

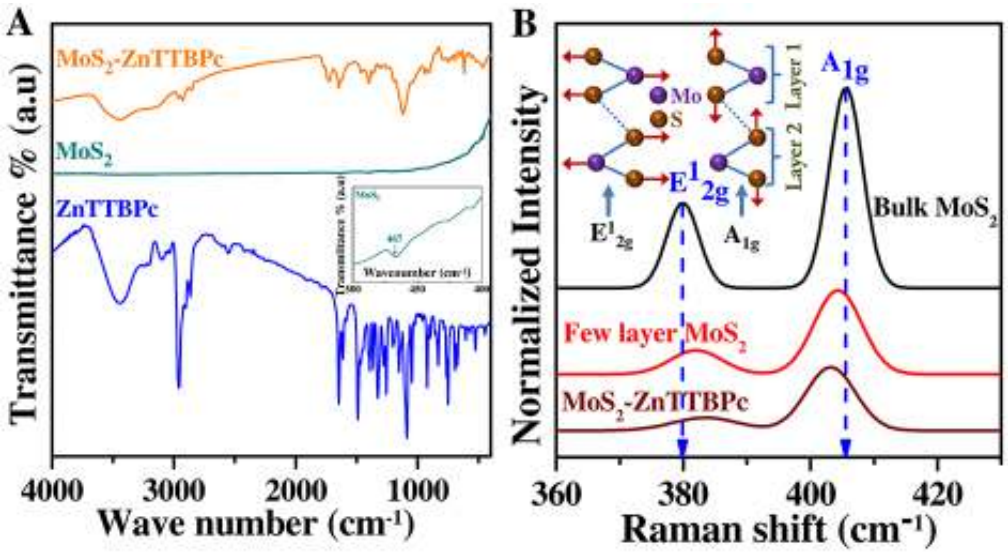

Figure 5.5.5: (A) $FTIR$ spectra of controlled-$ZnTTBPc$, controlled-MoS_2, and $MoS_2 - ZnTTBPc$ $(3:1)$ composite. The magnified view of $FTIR$ of controlled-MoS_2 (range : $500 - 400\,cm^{-1}$) is shown in the inset of (A). (B) Raman spectra of bulk MoS_2, few layers of MoS_2 (controlled- MoS_2), and $MoS_2 - ZnTTBPc$ $(3:1)$ composite. The vibration of E^1_{2g} and A^1_g is shown in the inset of (B).

Raman spectroscopy has been considered as a suitable diagnostic tool to determine the number of layers of MoS_2. In addition, it is also used to examine the formation of hybrid materials. Figure 5.5.5B represents the Raman spectra of bulk MoS_2, as prepared exfoliated MoS_2 layer ($controlled-MoS_2$) and $MoS_2 - ZnTTBPc$ composites with Gauss peak fitting. In all spectra, the two peaks are mainly observed, one is in-plane vibration modes (E^1_{2g}) and other is out of plane vibration (A_{1g}) modes [285] . The atomic displacements related to E^1_{2g} mode and A_{1g} is shown in inset of Figure 5.5.5B. The strong peak at $380.13\,cm^{-1}$ and $405.84\,cm^{-1}$ are shown by the bulk MoS_2. The few layers MoS_2 prepared by vigorous stirring shows the same peak at $382.06\,cm^{-1}$ and $404.56\,cm^{-1}$, respectively [286-288]. We noticed

a red shift of the in-plane vibration modes(E^1_{2g}) band as well as a significant blue shift of out of the plane vibration modes (A_{1g}) band and it is located at 383.34 and 403.2 cm^{-1}, respectively for $MoS_2 - ZnTTBPc$. The number of MoS_2 layer is estimated from the separation of energies (Δ) of two signatory Raman peaks. The calculated value of (Δ) for bulk MoS_2, MoS_2 few layer and $MoS_2 - ZnTTBPc$ nano composite are 25.71 cm^{-1}, 22.50 cm^{-1} and 19.86 cm^{-1} respectively which indicate that there are two layers of MoS_2 plane after sonicating MoS_2 particles. The monolayer of MoS_2 exists in $ZnTTBPc$ functionalized $MoS_2 - ZnTTBPc$ composites [285]. Thus $ZnTTBPc$ anchor on top of the MoS_2 surface without making any disturbance in its electronic configuration. Furthermore, the presence of $ZnTTBPc$ prevents the aggregation of MoS_2 and forms a monolayer of MoS_2 functionalized by $ZnTTBPc$. The AFM image also confirms the formation of monolayer $MoS_2 - ZnTTBPc$, as shown in Figure 5.5.6A

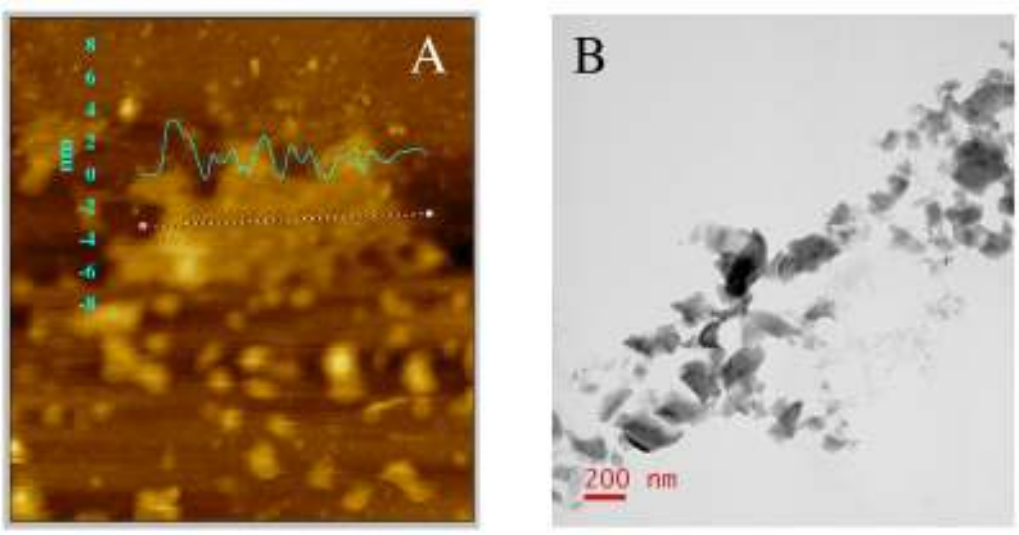

Figure 5.5.6: (A) AFM image of $MoS_2 - ZnTTBPc$ (3 : 1) composite films on a silicon wafer. (B) TEM image of $MoS_2 - ZnTTBPc$ (3 : 1) composite.

The AFM height image (cross-section analysis) shows the average thickness of $ZnTTBPc$ functionalized MoS_2 to be $\sim 2\,nm$, whereas the average thickness of a monolayer MoS_2 is $\sim 0.65\,nm$ and as reported by others. This confirms the formation of $MoS_2 - ZnTTBPc$ hybrid materials through the attachment of $ZnTTBPc$ on the MoS_2 plane via $\pi - \pi$ interaction.

5.6 Photocatalytic Activity of $MoS_2 - ZnTTBPc$ Composite

The photocatalytic reduction of $4 - NP$ in an excess amount of $NaBH_4$ has been considered as a protocol reaction in the last few years to study the photocatalytic performance of different semiconducting nanohybrid materials and metal nanoparticles [289] . The photocatalytic performance of $MoS_2 - ZnTTBPc\,(3:1)$, controlled-MoS_2, and controlled- $ZnTTBPc$ were assessed in same investigational situation towards the degradation of $4-NP$ solution under solar light (simulated) irradiation. The reduction of 4-NP was monitored through the $UV - Vis$ absorption measurement. In these absorption spectra, 4-NP shows its characteristics peak at $317\,nm$. The peak red shifted to $422\,nm$ in presence of excess $NaBH_4$ owing to the formation of phenolet ion and the colour of the solution become bright yellow [272]. The absorption intensity of phenolate ion remains unaltered in absence of any catalyst both the dark and under solar light irradiation, even though $NaBH_4$ is considered a strong reduction mediator ($Figure$ 5.6.1).

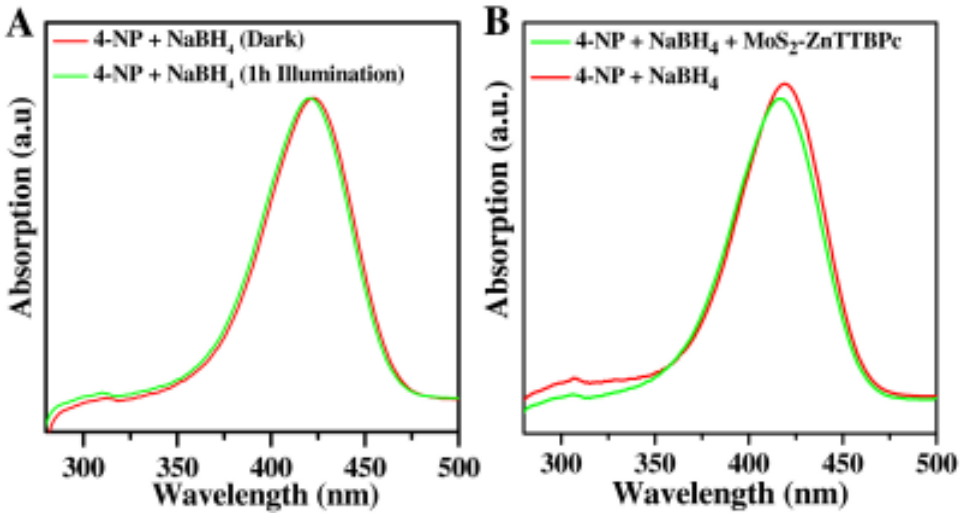

Figure 5.6.1: $UV - vis$ absorption spectra of $4 - NP$ and $NaBH_4$ solution (A) without catalyst under dark and simulated solar light illumination for 1 h (B) with and without $MoS_2 - ZnTTBPc$ $(3:1)$ composite under dark.

In presence of $MoS_2 - ZnTTBPc\,(3:1)$ catalyst the peak intensity decreased by 12% in $12\,min$ even in dark condition probably due to the surface adsorption of 4-NP in $MoS_2 - ZnTTBPc\,(3:1)$ nanocomposite [Figure 5.6.1B] [272, 290]. The large surface area and different vacancies presence in the composite acts as adsorption centre. The photocatalytic reduction of 4-NP starts immediately after exposure to light and the brilliant yellow colour of the solution vanishes gradually with time. Concurrently, a new peak appears at $346\,nm$ confirming the formation of $4-AP$, the basic component of paracetamol [291-293]. The $UV - vis$ absorption spectra of 4-NP in excess $NaBH_4$ reduced by $MoS_2 - ZnTTBPc\,(3:1)$ nano composite for different irradiation time is presented in Figure 5.6.2A. Where figure 5.6.2B and 5.6.2C represents the absorption spectra of 4-NP in excess $NaBH_4$ reduced by controlled $ZnTTBPc$ and controlled MoS_2 respectively.

It is observed that almost 91.6% of phenolet ions degraded within 56 min of the reduction process. Weakening of phenolate ion peak and appearing of amino phenol $(4-AP)$ related peak confirms that the mechanism is a photocatalytic reduction. The photocatalytic reduction efficiency was estimated as per the equation 2.4.4 [217, 222].

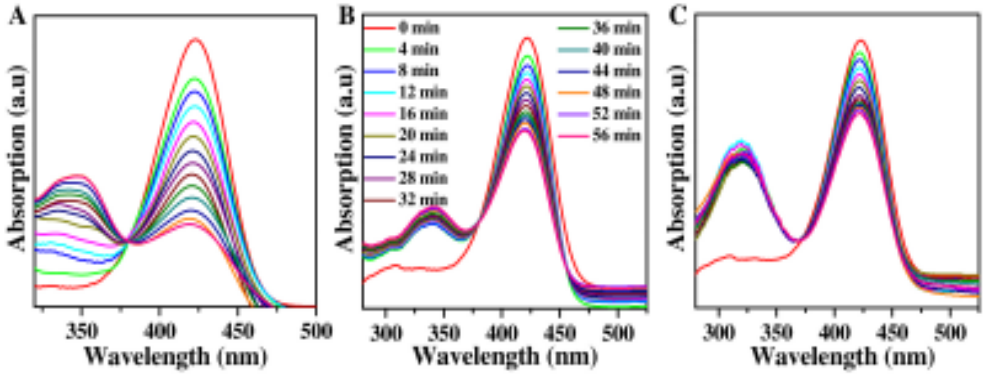

Figure 5.6.2: UV–vis absorption spectra of $4-NP$ and $NaBH_4$ solution with (A) $MoS_2-ZnTTBPc$ $(3:1)$ composite, (B) controlled-$ZnTTBPc$, and (C) controlled-MoS_2 for different time of simulated solar light illumination.

Figure 5.6.3A gives the significance comparison of reduction efficiency of MoS_2, controlled-$ZnTTBPc$ and $MoS_2-ZnTTBPC$ $(3:1)$ with respect to irradiation time. As can be seen in the figure, $MoS_2-ZnTTBPc$ $(3:1)$ showed a higher reduction efficiency (91.6 %), whereas the reduction efficiency of layered MoS_2 and $ZnTTBPc$ is 36.3% and 50.2% respectively, after light irradiation for 56 min. It is obvious that the presence of MoS_2 nanosheets could augment the photocatalytic reduction efficiency of $ZnTTBPc$. To give significant insight and get a further understanding of the photocatalytic reduction process, the photocatalytic reduction kinetics was explored. It is considered that for sufficiently low concentration, the photocatalytic re-

duction of 4-NP is a pseudo-first-order reaction [217, 220] , the kinetics of which can be expressed as

$$\ln\left(\frac{C}{C_0}\right) \;=\; -kt \tag{5.6.1}$$

where, k is denoted as the pseudo-first-order rate constant having unit min^{-1}. A linear variation of $ln\,(\frac{C_0}{C})$ with irradiation time (t) (Figure 5.6.3B) confirms the reduction kinetics is that of a pseudo-first order reaction and the slope of the straight line gives the value of k. Both controlled-$ZnTTBPc$ and MoS_2 exhibit somewhat a low photocatalytic activity with k values of $0.014\,min^{-1}$ and $0.010\,min^{-1}$ respectively. After efficient attachment of $ZnTTBPc$ on the layered surface of MoS_2, an evidently enhanced photocatalytic performance of $MoS_2 - ZnTTBPc\,(3:1)$ with a k value of $0.034\,min^{-1}$is observed.

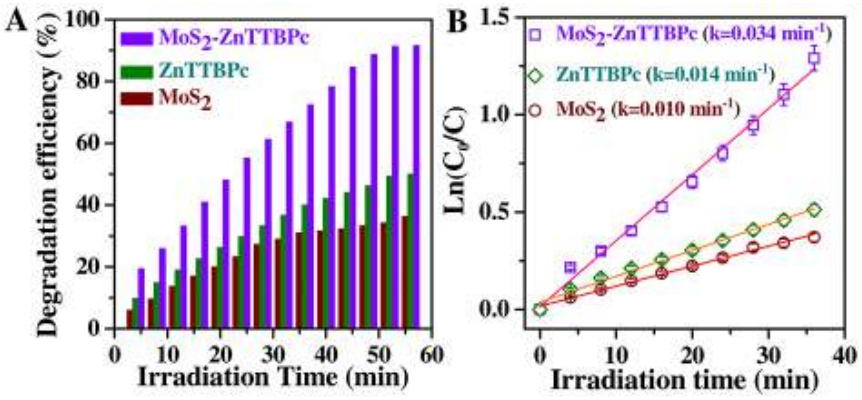

Figure 5.6.3: (A) Comparison of photodegradation efficiency as a function of time under simulated solar-light illumination for controlled-$ZnTTBPc$, controlled-MoS_2, and $MoS_2 - ZnTTBPc$ $(3:1)$ composite. (B) Plot of $ln(C_0/C)$ as a function of simulated solar-light irradiation time for the photocatalysis of $4-NP$ containing controlled-$ZnTTBPc$, controlled-MoS_2, and $MoS_2 - ZnTTBPc$ $(3:1)$ composite.

In order to study the effect of MoS_2 mass on the reduction efficiency of

the composite, we have evaluated the photocatalytic activity of all the composites. Under identical environment tye other four nano-composites, i.e. $MoS_2-ZnTTBPc\,(1:1)$, $MoS_2-ZnTTBPc\,(2:1)$, $MoS_2-ZnTTBPc\,(4:1)$ and $MoS_2-ZnTTBPc\,(5:1)$ meet the efficiency 62.3 and 64.5% respectively and are shown in Figure 5.6.4. It is interesting that all the composites demonstrate quite high photocatalytic efficiency compare to their components particularly and $MoS_2-ZnTTBPc\,(3:1)$ is the favoured choice of photocatalyst of $MoS_2-ZnTTBPc$ family.

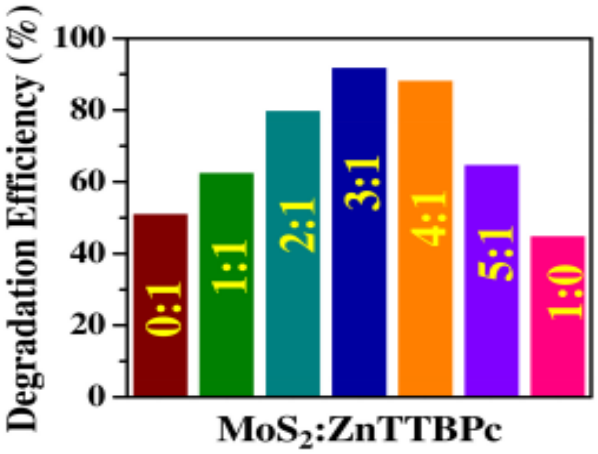

Figure 5.6.4: Comparison of the photo degradation efficiency with varying ratio of MoS_2 and $ZnTTBPc$ in the $MoS_2-ZnTTBPc$ composite.

It is evident that, a synergistic effect is involved among MoS_2 and $ZnTTBPc$ in the composite. Researchers have widely reported the synthesis of novel hybrid materials based on CNT, RGO and activated carbon and observed an enhanced photocatalytic performance due to synergistic effect of the individual components in the heterostructure materials [81, 206, 271, 272]. It is thus of immense significance to explore the synergy effect involved in the new set of $MoS_2-ZnTTBPc$ hybrid materials. As observed in Figure 5.6.3B,

both controlled-$ZnTTBPc$ and controlled-MoS_2 follow pseudo-first order reaction kinetics. Thus the degradation of $4-NP$ by MoS_2 and controlled-$ZnTTBPc$ are proportional to $\exp^{(-K_{MoS_2})t}$ and $\exp^{(-K_{ZnTTBPc})t}$ respectively, where, K_{MoS_2} and $K_{ZnTTBPc}$ are the degradation/reduction rate constant of MoS_2 and controlled-$ZnTTBPc$ respectively. Thus in the hybrid material the reduction of $4-NP$ should depend synergistically on the intriguing properties of the individual components and the degradation of $4-NP$ by the $MoS_2-ZnTTBPc$ ought to be proportional to the product of the individual components ($\exp^{(-K_{MoS_2})t} \times \exp^{(-K_{ZnTTBPc})t}$). Although several reports on the synergistic effect of the MoS_2-based composite are available but effective synergy factor was not reported. Thus the beneficial effect can be estimated by the synergy factor (R) for $MoS_2-ZnTTBPc$ can be attributed by considering its controlled counterpart and R can be determined by the relation as [294]

$$R = \frac{K_{MoS_2-ZnTTBPc}}{K_{MoS_2}+K_{ZnTTBPc}} \tag{5.6.2}$$

This yielded a synergy factor of 1.42 for the $MoS_2-ZnTTBPc$ composite.

The photocatalytic reduction of aromatic nitro compounds like 4-NP depends on several factors: adsorption of the reactants on the surface of the optical materials, broadband absorption of photon by the catalyst, presence of catalytic active sites, exciton formation and dissociate to free carriers and subsequently transportation to the active sites. In $MoS_2-ZnTTBPc$ compound, presence of highly active nanoscale dimension MoS_2 monolayer offers additional sites for the photocatalytic reduction of 4-NP. It also increases the optical absorption in the composite which facilities the creation of charge

carriers and efficient reduction of the nitrophenolate ion. Under the illumination of simulated solar light, excitons are generated both in MoS_2 and $ZnTTBPc$, which dissociates into free electron and hole at the conduction and valence band of both in MoS_2 and $ZnTTBPc$. Due to the favorable band position [294] the electrons transfer from the conduction band of $ZnTTBPc$ to the conduction band of MoS_2, whereas, the holes transfer from the valence band of MoS_2 to the valence band of $ZnTTBPc$. The good separation of electrons at the conduction band of MoS_2 and the holes at the valence band of $ZnTTBPc$ reduces the electron-hole recombination probability in the composite under light illumination.

Figure 5.6.5: Mechanism of photocatalytic reduction of $4-NP$ using $MoS_2-ZnTTBPc$ $(3:1)$ under solar light illumination.

On the other hand, in presence of $NaBH_4$, the 4-NP creates phenolate ions which reduce to $4-AP$ by accepting the electrons from MoS_2 sheets.

The anticipated mechanism for photocatalytic reduction of $4-NP$ using $MoS_2-ZnTTBPc$ under solar light illumination is presented in Figure 5.6.4. The strong synergetic effect between MoS_2 and $ZnTTBPc$ extensively boosts the photocatalytic activity of $MoS_2 - ZnTTBPc$ composites. Further, recycle tests were employed to establish the stability of $MoS_2-ZnTTBPc\,(3:1)$ photocatalyst. Reduction efficiency of the photocatalyst is not remarkably changed after five successive recycle uses under identical experimental condition (Figure 5.6.6A)

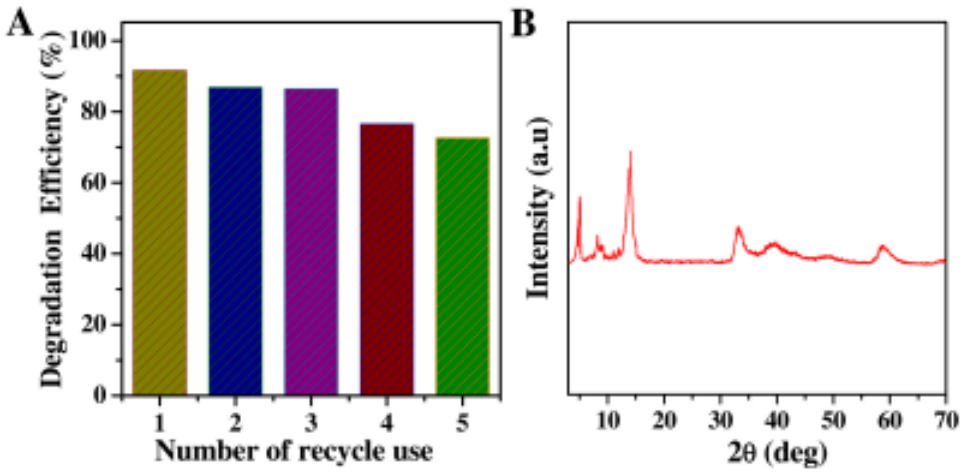

Figure 5.6.6: (A) Photodegradation efficiency of $MoS_2 - ZnTTBPc$ $(3:1)$ composite for different cycle. (B) The XRD pattern of $MoS_2 - ZnTTBPc$ $(3:1)$ composite after five cycles of reduction of $4-NP$.

The stability of the composite is further confirmed by the XRD measurement of the composite after completing five cycles of $4-NP$ reduction (figure 5.6.6B). No significant change in the crystalline structure of $MoS_2 - ZnTTBPc\,(3:1)$ is observed after recycle used, confirms the stability of the photocatalyst.

5.7 Conclusion

Herein, we have shown a very convenient process for the scalable synthesis of MoS_2 functionalized by $ZnTTBPc$ which is considered an electron donor material. The $MoS_2 - ZnTTBPc$ nanocomposite has been synthesized successfully by the sonochemical technique and the hybrid material has been characterized by means of different techniques such as XRD, $UV-Vis$, PL, $TCSPC$, Raman and $FTIR$ spectroscopy. The occurrence of charge transfer from $ZnTTBPc$ to MoS_2 has been jointly authenticated by the steady-state PL and $TCSPC$ study. The energy transfer efficiency as high as 90% for the $MoS_2 - ZnTTBPc\,(3:1)$ composite. Raman study gives sufficient evidence of existence mono-layer MoS_2 in the $MoS_2 - ZnTTBPc\,(3:1)$ composite. It can be stated as $ZnTTBPc$ effectively prevents the aggregation of MoS_2 and provides the monolayer of MoS_2, which makes it a potential optoelectronic material.

The positive synergetic effect among $ZnTTBPc$ and single layered-MoS_2 sheets act as co-catalyst on the photocatalytic activity. In the composite, the favorable band alignment of MoS_2 and $ZnTTBPc$ facilitates better charge transfer at the interface subsequently suppress recombination probability of the photo generated charge carriers. Plenty of active adsorption sites available on the $2D$ surface of MoS_2 also efficiently acts as photocatalytic reaction centres. The present study opens new possibilities to functionalize MoS_2 by the donor materials where single layer-MoS_2 acts as acceptor. It could thus present a promise as a new photocatalyst towards removing different aquatic pollutants and other optoelectronic devices.